Realization of a Large J_2 Quasi-2D Spin-Half Heisenberg System: Li$_2$VOSiO$_4$

H. Rosner,[1,*] R. R. P. Singh,[1] W. H. Zheng,[2] J. Oitmaa,[2] S.-L. Drechsler,[3] and W. E. Pickett[1]

[1]*Department of Physics, University of California, Davis, California 95616*
[2]*School of Physics, University of New South Wales, Sydney NSW 2052, Australia*
[3]*Institut für Festkörper- und Werkstofforschung Dresden e.V., Postfach 270116, D-01171 Dresden, Germany*
(Received 17 September 2001; published 23 April 2002)

Exchange couplings are calculated for Li$_2$VOSiO$_4$ using the local-density approximation (LDA). While the sum of in-plane couplings $J_1 + J_2 = 9.5 \pm 1.5$ K and the interplane coupling $J_\perp \sim 0.2$–0.3 K agree with recent experimental data, the ratio $J_2/J_1 \sim 12$ exceeds the reported value by an order of magnitude. Using geometrical considerations, high temperature expansions and perturbative mean field theory, we show that the LDA-derived exchange constants lead to a remarkably accurate description of the properties of these materials including specific heat, susceptibility, Néel temperature, and NMR spectra.

In many recently discovered magnetic materials the determination of exchange constants, without input from electronic structure calculations, has proven very difficult and has often led to wildly incorrect parameter values. The interplay of geometry and quantum chemistry has yielded many surprises which could not have been anticipated without a full calculation. Examples are the recently discovered vanadates CaV$_4$O$_9$ [1] and CaV$_3$O$_7$ [2], for which the dominant exchange interactions were resolved and a good understanding of the material properties obtained only after analyses of electronic structure calculations were carried out.

Frustrated square-lattice spin-half Heisenberg antiferromagnets with nearest neighbor exchange J_1 and second neighbor exchange J_2 have received considerable attention recently. The properties of the model with $J_2 = 0$ (or $J_1 = 0$) are well understood [3]. The large J_2 limit of the model is a classic example of quantum order by disorder [4,5], where at the classical level the two sublattices order antiferromagnetically but remain free to rotate with respect to each other. This degeneracy is lifted by quantum fluctuations leading to collinear magnetic order in a columnar pattern. At intermediate J_2/J_1 there is strong evidence for a spin-gap phase, though the nature of this phase is not fully resolved yet [6].

While there has been tremendous theoretical interest in these models, there were no known experimental realizations for intermediate to large J_2/J_1, until the investigation of Li$_2$VOSiO$_4$ by Melzi *et al.* [7,8]. Studying the splitting patterns of the ^{7}Li NMR spectra, these authors presented strong evidence for columnar order [7]. Combining several experiments they derive [8] exchange couplings (with $J_2/J_1 \sim 1.1$) well into the region where model calculations find columnar order.

However, several puzzling pieces in that excellent and detailed study remain: (i) The ratio of exchange constants was not well determined from the susceptibility and specific heat data; we will present electronic structure and many-body calculations to show that their estimate $J_2/J_1 \approx 1$ [8] is not justified by the data. (ii) The

estimated $T = 0$ moment was anomalously small for a system well inside the columnar ordered phase. Taking into account the antiferromagnetic interplane coupling, we propose that the NMR derived moment is small due to a cancellation of hyperfine fields from neighboring planes. (iii) The order parameter exponent β at the transition was estimated to be $\beta \approx 0.25$, which is intermediate between 2D Ising and typical 3D exponents. We will show that the interplane exchange constants differ from the largest ones by less than 2 orders of magnitude. Thus a strong crossover between 2D and 3D behavior could be expected. (iv) The Néel temperature was nearly field independent up to a field of 9 T. We will argue that our increased estimate of J_2 leads to a larger saturation field and that combined with nonmonotonic dependence of Néel temperature on field implies that the experimental results are not anomalous.

Our study of the material Li$_2$VOSiO$_4$ consists of a two band tight-binding (TB) model fit to the LDA band structure, which is then mapped onto a Heisenberg model with in-plane (J_1 and J_2) and interplane ($J_\perp$) exchange constants. Furthermore, we develop high temperature series expansions and perturbative mean-field theory for the uniform susceptibility and specific heat of the $J_1 - J_2$ model and make quantitative comparisons with experiments.

Li$_2$VOSiO$_4$ crystallizes in the tetragonal $P4/nmm$ system containing two formula units per cell with $a = 6.3682$ Å and $c = 4.449$ Å [9] (see Fig. 1). The magnetically active network of spin half V^{4+} ions is built up by [VOSiO$_4$]$^{2-}$ layers of VO$_5$ square pyramids sharing corners with SiO$_4$ tetrahedra, intercalated with Li ions. The structure of the V^{4+} square network suggests that both the nearest neighbor (NN) and the next nearest neighbor (NNN) in-plane coupling should be significant, although it is at best difficult to decide from general considerations which one is dominant. NN coupling is favored by the existence of two exchange channels and shorter distance, NNN coupling profits from the "straight" connection between pyramids pointing in the same direction.
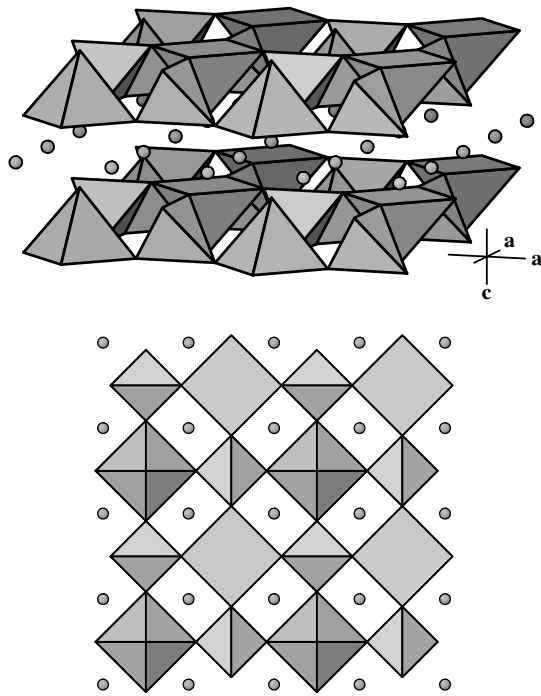
FIG. 1.   Perspective view (upper panel) of the crystal structure of Li_2VOSiO_4 and projection along [001] (lower panel). The VO_5 pyramids (large diamonds) share the corners of the basal planes with SiO_4 tetrahedra (small diamonds). The Li^+ ions are indicated by circles.

In order to obtain a realistic and reliable hopping part of a TB Hamiltonian, band structure calculations were performed using the full-potential nonorthogonal local-orbital minimum-basis scheme [10] within the local density approximation (LDA). In the scalar relativistic calculations we used the exchange and correlation potential of Perdew and Zunger [11]. $V(3s, 3p, 4s, 4p, 3d)$, $O(2s, 2p, 3d)$, $Li(2s, 2p)$, and $Si(3s, 3p, 3d)$ states, respectively, were chosen as the basis set. All lower lying states were treated as core states. The inclusion of $V(3s, 3p)$ states in the valence states was necessary to account for non-negligible core-core overlaps. The O and Si $3d$ as well as the Li $2p$ states were taken into account to increase the completeness of the basis set.

The results of the paramagnetic calculation (see Fig. 2) show a valence band complex of about 10 eV width with two bands crossing the Fermi level. These two bands, due to the two V per cell, are well separated by a gap of about 3 eV from the rest of the valence band complex and show mainly V $3d_{xy}$ and minor $O(2)$ $2p_{x,y}$ character (oxygens of the basal plane of the VO_5 pyramid) in the analysis of the corresponding orbital-resolved partial densities of states (not shown). The valence bands below the gap and above the Fermi level have almost pure oxygen and vanadium character, respectively. The contribution of Li and Si states is negligible in the energy region shown.

The narrow bands at the Fermi level (see Fig. 2, lower panel) are half filled. Therefore, strong correlation effects
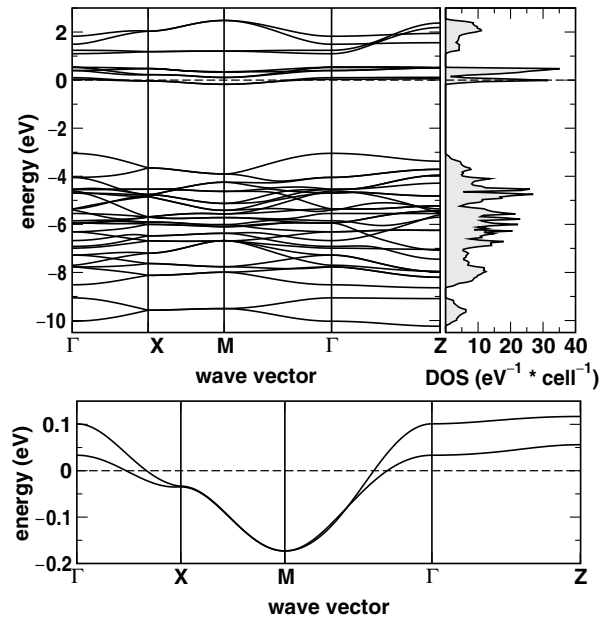
FIG. 2.   Band structure and total density of states for Li_2VOSiO_4 (upper panel) and the zoomed bands closest to the Fermi level (lower panel). The Fermi level is at zero energy. The notation of the symmetry points is as follows: $X = (100)$, $M = (110)$, $Z = (001)$.

can be expected which explain the experimentally observed insulating ground state. Because the low-lying magnetic excitations involve only those orbitals with unpaired spins corresponding to the two half-filled bands, we restrict ourselves to a two band TB analysis.

The dispersion of these bands (see Fig. 2, lower panel) has been analyzed in terms of NN transfer t_1 and NNN transfer t_2 within the [001] plane (see Fig. 1 lower panel) and NN hopping $t_\perp$ between neighboring planes. Then, the corresponding dispersion relation of the related 2×2 problem takes the form

$$E(\vec{k}) = \varepsilon_0 + 2t_2[\cos(k_x a) + \cos(k_y b)] \\ \pm 4t_1 \cos(k_x a/2)\cos(k_y b/2) + 2t_\perp \cos(k_z c). \quad (1)$$

The assignment of the parameters has been achieved by two numerically independent procedures: by straightforward least square fitting of the two bands in all directions and by using the energy eigenvalues at different selected high symmetry points. The results are shown in Table I. The errors can be estimated about 5% for the in-plane transfers and 15% for the interplane term from the differences of both mentioned above fitting procedures due to the influence of higher neighbors. The very good agreement of the TB fit with the LDA bands justifies *a posteriori* the restriction to NN and NNN couplings only.

The resulting transfer integrals enable us to estimate the relevant exchange couplings, crucial for the derivation and examination of magnetic model Hamiltonians of the spin-1/2 Heisenberg type:

$$H_{\mathrm{spin}} = \sum_{ij} J_{ij} \vec{S}_i \cdot \vec{S}_j. \tag{2}$$

In general, the total exchange J can be divided into an antiferromagnetic and a ferromagnetic contribution $J = J^{AFM} + J^{FM}$. In the strongly correlated limit, valid for typical vanadates, the former can be calculated in terms of the one-band extended Hubbard model $J_i^{AFM} = 4t_i^2/(U - V_i)$. The index i corresponds to NN and NNN, U is the on-site Coulomb repulsion, and V_i is the intersite Coulomb interaction. Considering the fact that the VO_5 pyramids are not directly connected, but via SiO_4 tetrahedra, ferromagnetic contributions J^{FM} are expected to be small. For the same reason, the intersite Coulomb interactions V_i should be small compared with the on-site repulsion U. From LDA-DMFT(QMC) studies [12] and by fitting spectroscopic data to model calculations [13], $U \sim 4$–5 eV is estimated for typical vanadates. Therefore, we adopt $U = 4$ eV and $U = 5$ eV as representative values to estimate the exchange constants and their sensitivity to U. The calculated values for the exchange integrals are given in Table I.

Comparing our calculated exchange couplings with the experimental findings [8], we find excellent agreement for the sum $J_1 + J_2 = 9.5 \pm 1.5$ K [14] of the in-plane couplings, reported from susceptibility data [8] to be $J_1 + J_2 = 8.2 \pm 1$ K. In contrast, we find a ratio $J_2/J_1 \sim 12$ which exceeds the experimentally derived ratio in Ref. [8] $J_2/J_1 \sim 1.1 \pm 0.1$ by an order of magnitude.

In order to investigate the consistency of our calculated parameters with the experimental data, we turn to high temperature expansions [16] for the $J_1 - J_2$ Heisenberg model. Series expansion coefficients are calculated complete to order β^9, for arbitrary ratio of J_2/J_1 for the uniform susceptibility (χ) and the internal energy. From the latter, the series coefficients for the specific heat (C) are readily obtained. Standard series extrapolation methods are then used to get the temperature dependent susceptibility and specific heat. We have also developed a perturbative mean-field theory, analogous to chain mean-field theories [17], which for small J_1/J_2 allows us to calculate the χ accurately down to $T = 0$. However, since the very low temperature behavior is not relevant to the comparison with experimental data we defer discussion of the perturbative mean-field theory to a more extensive paper [18].

The experimental susceptibility data do not show a Curie-Weiss regime at high temperatures. Thus any effort to fit the data both near room temperature and at temperatures of order J will fail. Since we are interested

in the behavior of the system at low temperatures, we confine attention to the temperature region $T < 20$ K (which still goes more than twice above the Curie-Weiss temperature). We find that fitting of the susceptibility and specific heat data is not sensitive to J_2/J_1 ratio. In looking for consistency between the LDA calculations and the experimental data, we adopt the following strategy. In LDA, the ratio of exchange constants should be best determined as the parameter U cancels out. Hence, we fix $J_2/J_1 = 10$ consistent with LDA. We then vary g and J_2 to obtain the best fit to the susceptibility data. This is obtained for $J_2 = 6.1$ K, 20% smaller than the lower bound of the LDA calculation. The agreement is still remarkable for an *ab initio* calculation.

The susceptibility fit, as shown in Fig. 3, is excellent. The specific heat data are now compared with theory with *no adjustable parameters*. This is shown in the inset of the figure. The agreement is remarkable. We also applied the same fitting procedure for $J_2/J_1 = 1$ the value proposed in Ref. [8]. The agreement is very poor [18]. Thus, although the susceptibility and specific heat data do not allow us to fix the exchange integrals unambiguously, they are quite consistent with small J_1/J_2 ratio as found in LDA, and inconsistent with $J_2 \approx J_1$.

Accurate determination of the J_2/J_1 ratio can come from measurements of the spin-wave dispersion throughout the Brillouin zone. The dispersion has been calculated by several authors [5,19]. Throughout the columnar phase, i.e., independent of J_2/J_1 there are gapless excitations at $(0,0)$, $(0,\pi)$, $(\pi,0)$, and (π,π). However, the high energy spin-wave dispersion and the X-Y asymmetry of the spectra, which comes from ferromagnetic alignment along one direction and antiferromagnetic along the other, depends sensitively on J_2/J_1.
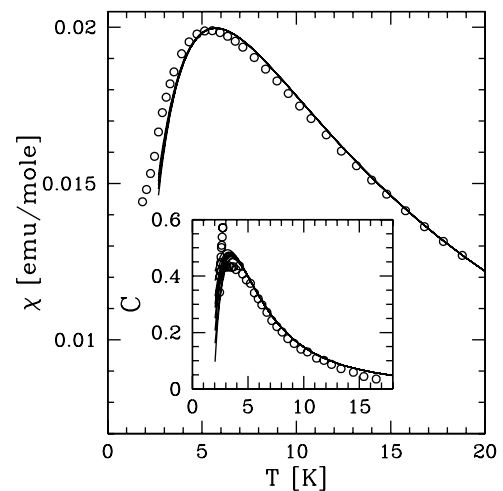
FIG. 3. Calculated (solid lines) susceptibility χ and specific heat C (inset) for $J_2 = 6.1$ K, $g = 1.9$, and $J_2/J_1 = 10$. The different curves correspond to different Padé approximations and demonstrate the range of validity of the HTE. The experimental data from Ref. [7] are plotted as circles.

TABLE I. Transfer integrals of the two-band TB model and the corresponding exchange couplings for different values of the Hubbard U.

t_1 (meV)	t_2 (meV)	$t_\perp$ (meV)	U (eV)	J_1 (K)	J_2 (K)	$J_\perp$ (K)
8.5	29.1	-4.8	4	0.83	9.81	0.27
			5	0.67	7.85	0.22

One of the most puzzling aspects of the experimental results [8] is the small moment of $0.24\mu_B$ at $T = 0$, obtained from the NMR split patterns. In contrast, the moment of the square-lattice Heisenberg model is well known to be $\approx 0.6\mu_B$ [15]. Taking into account the considerable antiferromagnetic interplane coupling $J_\perp$ resulting from our calculation, a part of the discrepancy can be understood: The Li nuclei sit between two pairs of inequivalent V atoms, which results in a partial cancellation of the hyperfine fields from antiferromagnetically ordered NN and NNN V sites (see Fig. 4). This partial cancellation does not change the arguments of Melzi *et al.* for the pattern of line splitting (including intensities) and its relation to columnar order because the ordering pattern inside the planes remains the same. However, it leads to a reduction in the effective hyperfine coupling and hence to an enhancement of magnetic moment derived from the line shift. Taking into account the calculated two center overlap integrals for Li and NN and NNN V 3*d* orbitals, respectively (see Fig. 4) a crude estimate from Slater-Koster integrals suggests that the NMR split would be reduced by an additional factor of about 2. This results in a moment of about $0.5\mu_B$, much closer to the value expected for the 2D Heisenberg model.

We now turn to the interplane couplings and the measurements of the Néel temperature, T_N. Applying the expression $T_N \approx 0.36J_\perp\xi^2(T_N)$ [3,20] (ξ is the in-plane correlation length), to our LDA calculated exchange constants, leads to the estimate $T_N \approx 3.6 \pm 0.4$ K, which is remarkably close to the experimental value of 2.8 K. Furthermore, the saturation field for our calculated exchange constants is about 30 T, which is much bigger than the 9 T field applied by Melzi *et al.* [21]. The Néel temperature should go to zero at the saturation field. However, we note that due to suppression of spin fluctuations the Néel temperature can increase slightly with field, as happens in the purely 2D model. Thus, the experimental result of very weak field dependence of the Néel temperature up to 9 Tesla is consistent with our expectations. The appreciable but still small 3D couplings should also give rise to 3D

critical behavior at the finite temperature transition with strong crossover effects. These results on the field dependence of the Néel temperature and the critical behavior at the transition in weakly coupled quasi 2D Heisenberg systems deserve further theoretical attention.

To summarize, we have used the LDA to calculate exchange constants for the compound Li_2VOSiO_4 and developed numerical studies for the corresponding Heisenberg model to show remarkable consistency with experimental properties. Electronic structure calculations on the closely related material Li_2VOGeO_4 will be presented in a forthcoming publication [18]. The key differences are the considerably smaller J_2/J_1 ratio and coupling to higher neighbors in Li_2VOGeO_4. Finally, these materials have a substantial 3D coupling, and it would be interesting to find one that does not.

FIG. 4. Sketch of the different magnetic environments for the ^{7}Li NMR. The Li and V sites are represented by black and gray circles, respectively. The arrows indicate the direction of the V spin. Full lines symbolize the stronger interaction with the NN vanadium sites, dashed lines the weaker interaction with the NNN vanadium sites. The different environments cause (a) no NMR shift due to complete moment-cancellation; (b) up or down shift with partial moment-compensation.

*Corresponding author: helge@physics.ucdavis.edu
[1] W. E. Pickett, Phys. Rev. Lett. **79**, 1746 (1997).
[2] M. A. Korotin *et al.,* Phys. Rev. Lett. **83**, 1387 (1999).
[3] S. Chakravarty, B. I. Halperin, and D. R. Nelson, Phys. Rev. Lett. **60**, 1057 (1998).
[4] E. Shender, Sov. Phys. JETP **56**, 178 (1982).
[5] P. Chandra, P. Coleman, and A. I. Larkin, Phys. Rev. Lett. **64**, 88 (1990).
[6] O. P. Sushkov, J. Oitmaa, and W. H. Zheng, Phys. Rev. B **63**, 104 420 (2001).
[7] R. Melzi *et al.,* Phys. Rev. Lett. **85**, 1318 (2000).
[8] R. Melzi *et al.,* Phys. Rev. B **64**, 024409 (2001).
[9] P. Millet and C. Satto, Mater. Res. Bull. **33**, 1339 (1998).
[10] K. Koepernik and H. Eschrig, Phys. Rev. B **59**, 1743 (1999).
[11] J. P. Perdew and A. Zunger, Phys. Rev. B **23**, 5048 (1981).
[12] K. Held *et al.,* Phys. Rev. Lett. **86**, 5345 (2001).
[13] T. Mizokawa and A. Fujimori, Phys. Rev. B **48**, 14 150 (1993); J. Zaanen and G. A. Sawatzky, J. Solid State Chem. **88**, 8 (1990).
[14] The specified error results from the uncertainty of U and the errors for t_1 and t_2 from the TB fit.
[15] C. J. Hamer, W. H. Zheng, and J. Oitmaa, Phys. Rev. B **50**, 6877 (1994).
[16] N. Elstner *et al.,* Phys. Rev. Lett. **75**, 938 (1995).
[17] D. J. Scalapino, Y. Imry, and P. Pincus, Phys. Rev. B **11**, 2042 (1975).
[18] H. Rosner *et al.,* (to be published).
[19] A. F. Barabanov and O. A. Starykh, JETP Lett. **51**, 311 (1990).
[20] For large J_2 it is appropriate to consider only J_2 to determine the in-plane ξ, which is well known from previous studies; see, e.g., Ref. [3].
[21] Taking our fitted value of $J_2 = 6.1$ K, we estimate $T_N \approx 2.6$ K and a saturation field ≈ 20 T.